Modeling of oxide inclusions in steel casting

Modeling of oxide inclusions in steel casting

R Donahue, R Hardin, and C Beckermann

Department of Mechanical Engineering, University of Iowa, 3131 Seamans Center, Iowa City, IA 52242, USA

becker@engineering.uiowa.edu

Abstract. A model is presented that predicts the amount and location of oxide inclusions in steel castings. A number and size distribution of inclusions, defined about a mean diameter, enters the casting system at its inlet during the filling process and are transported to their final locations in the casting. Model parameters for inclusion density, drag and wall friction are used to calculate the motion and locations of the oxide particles. Model results are presented to study the effects of casting shape and surface orientation on the final inclusion locations and distributions within castings. These results are compared with inclusion tracking experiments where the geometry of the gating system and orientation of casting cope surfaces affect the final distribution of inclusions in the castings. Measured and simulated inclusion area percent coverage, inclusion count and mean diameter are compared for a range of modelling parameters and inclusion size distributions. The size and number distribution at the casting system inlet, and other model parameters, are determined which provide the best agreement between measured and simulated inclusion area, count, and size.

1. Introduction

Oxide inclusions in steel castings are estimated to contribute 20% to the cost of a casting due to the costs of removing them and repairing the casting [1]. They are also a frequent cause of premature failure of steel castings when not detected during production. There are numerous sources of oxides such as the ladle lining and poorly deoxidized melt, and many casting process variables can affect the levels of oxides in steel castings. The cleanliness of the melt can vary from heat to heat, so called dirty heat versus clean heat, due to poor control of the melt practice. Considering all the sources of oxide inclusions, reoxidation inclusions, formed during pouring of the metal into the mold, are a common cause of inclusion defects in steel castings, if not the most common. Reoxidation inclusions form when deoxidized steel comes into contact with oxygen during mold filling. They are reported to make up 83% of oxide inclusions in low-alloy steel castings and 48% of inclusions found in high-alloy steel castings [2]. Reoxidation of the steel during pouring can be minimized by employing well designed gating systems. Much research has been performed for over 50 years to establish rules for gating castings. However, the design of gating systems is still more of an art than a science. Instead of investigating source of the inclusions, like reoxidation, the present paper focuses on modeling the transport of inclusions throughout gating and casting systems and their final locations.

One of the authors has previously modeled reoxidation inclusions originating on the free melt surface with their growth controlled by oxygen transfer from the atmosphere and their motion and agglomeration [3]. This paper presents the results from a model where the number and size distribution of inclusions, defined about a mean diameter, enters the casting system at its inlet during the filling. Generation of

inclusions in the casting system by reoxidation is not considered. Inclusions enter the casting system from the ladle and are transported to their final locations in the casting using the inclusion motion model presented in [3]. Model results are compared to a series of casting experiments. The experiments are designed to investigate the control of oxide inclusions in steel casting using simple geometries to affect their transport and final locations. It is assumed that inclusions measured in the experiments either came directly from the ladle or were generated in the pouring cup. This assumption is based on an experimental investigation [4] using the melt and pouring practice used in the experiments presented here. In [4] ceramic foam filters were positioned at several locations in the casting system: at the inlet to the pouring cups filtering the stream, at the exit of the pouring cups (top of down sprue), at the base of the downsprue, and at the ingate to the casting. By pouring repetitions of experiments for the various filter location cases, it was found that a negligible number of inclusions was generated in the gating system. A range of "good" and "poor" gating systems were used as described in [4]. Inclusions measured in the experiments either came directly from the ladle or were generated in the pouring cup.

Therefore the model applied here assumes a distribution of inclusions entering the casting system only at the pouring cup with no growth or agglomeration. The model predicts the amount of area coverage and final locations of oxide inclusions in steel castings. The primary objectives of the present study are to determine the number of inclusions, their size distribution and other model parameters that give best agreement between the model and the measurements. Percent area coverage of inclusions, average inclusion indication size and number of indications on the casting surfaces are used to determine the agreement.

2. Description of Model and Analysis of Simulation Results

The model used in this paper was developed based on previous work [3,5]. It is referred to as a "dross" model as it applies to liquid metals forming dross inclusions (i.e., ductile iron [5], nickel-aluminum bronze and aluminum alloys) when the liquid metal surface is exposed to oxygen. In the case of this model, inclusions were determined to primarily come from the ladle used to fill the casting. In all experiments discussed and simulated here, ASTM A216 WCB steel was poured at the University of Northern Iowa Metal Casting Center using a 300-pound lip-pour ladle. During the holding of the steel prior to pouring, inclusions accumulated on the surface of the ladle due to reaction with the air, and convection and buoyancy effects bring them to the top surface. While efforts were made to de-slag and remove the inclusions from the melt surface prior to pouring, inclusions remained on the melt surface and entered the castings via the inlet stream. Upon entering the casting with the filling flow, the inclusions are transported with the flow under the effects of buoyancy and drag to their final locations in the solidifying casting.

Because of the observations discussed above, the current model assumes the sole source of inclusions is at the inlet to the casting system having; 1) a prescribed total number of inclusions N_{inc} entering the casting system during filling, and 2) a size distribution ranging from 50% to 150% about a prescribed mean inclusion diameter d_{inc}. The inclusions are assumed to be spheres. All other aspects of the model for calculating the motion and final locations of the inclusions are as described in [3] and [5] except that agglomeration is not considered here. Therefore, additional parameters used in the inclusion equation of motion [3] are the inclusion density ρ_{inc} and the wall slip coefficient λ_{inc}. As in [3] and [5], the model has been developed within the framework of a commercial casting simulation code.

The lip pour ladle filling stream was simulated as realistically as possible. As the lip pour ladle is tilted progressively to pour castings, the inlet stream falls at an angle from the lip to the inlet of the casting system. In the software used, an inlet is defined in an orientation aligned with the gravitational vector (the vertical direction) in order to define the inlet pouring stream. An angled stream such as that from a lip pour ladle is difficult to define in the software. To generate a more realistic lip pour stream than using the vertically aligned inlet, the inlet is aligned vertically, and the inlet filling stream flows through a channel designed to generate a stream falling at an angle before entering the pouring cup at the top of the downsprue.

The inclusion area coverage and number are measured in the experiments. To compare the simulation results to the experiments, the inclusion simulation results must be quantitatively evaluated to determine the inclusion area coverage and inclusion number on the casting surfaces as well. The inclusions on the experiment casting surfaces are observed to be pancake-shaped, while the inclusions formed in the simulations are spheres. To make the comparison to the measurements, the spherical inclusions on the surfaces of the simulated castings are converted to flattened disks having the same volume. A flattened inclusion has a larger diameter than a sphere of the same volume. Based on an experimental study of inclusions removed from the surfaces of castings, it was found that the actual flattened inclusions had an average diameter 1.7 times the diameter of a sphere having the same volume. To analyze the simulated inclusion size distributions, an image of the inclusion distribution result on the surface analyzed is made in the software's post-processor with the inclusions scaled to their true size. To model the flattened shape of the inclusions observed in the experiments, these spherical results are converted to flat disk diameters by increasing their size using a factor of 1.7 in the post-processor. Then the image of the flattened inclusions is converted to a binary image and analyzed using the software *ImageJ* [6]. In *ImageJ* the particle analysis feature is used to calculate the inclusion area coverage on the casting surface, inclusion count/number and the average diameter.

3. Experimental Inclusion Measurements

The objective of the experiments was to generate inclusions and produce flow patterns in various casting geometries to study the effects of casting shape and surface orientation on the final inclusion locations and distribution within the casting. This experimental data is generated to compare results with the model described above, and will provide data for calibration and validation of the model.

The experiments were quantitatively analyzed, and inclusions were measured. The as-cast cope surfaces of the experiments are first cleaned with a wire brush and then media blasted. The cleaning exposes inclusion pits since the inclusions are removed by media blasting. The casting surfaces are inspected and the inclusion pits are marked. The marked areas of inclusions are digitally photographed. These digital images are converted to binary images. The binary images are quantitatively analyzed using image analysis software [6] in the same way the simulation results are analyzed to measure the inclusion area, inclusion count and average inclusion diameter on the casting surfaces.

The six experiment cases presented here are shown in Figure 1. Dimensions of the experimental castings and other geometric features are provided. The first experiment (case A) shown in Figure 1(a) has two inclined surfaces at angles of 55° and 30° and is referred to as an "Angled Cope" casting. The second experiment case B is shown in Figure 1(b) and is an experiment with flow around a circular core. The next two cases C1 and C2 are plates inclined by 30° and 60° as seen in Figure 1(c). These cases are similar to the "Angled Cope" experiment case except that the inclination angles are split into separate cases. The last two experiments, having a ring flow pattern during filling are shown in Figure 1(d). In both experiments the filling flow enters the ingate and circles counter clockwise as viewed from above. In one "Ring Flow" experiment a recessed notch is positioned on top of the casting (case D1) and in the other a dirt trap is positioned on top of the casting. The dirt trap feature is essentially the opposite of the notch case, creating a cavity above the casting's cope surface. The notch and the dirt trap have similar dimensions. Chills are used in all cases as discussed below.

The experiments were designed so that the castings would capture any and all inclusions possible for measurement. In steel castings, inclusions can be removed from castings during filling, if the flow carries them into feeders. It was determined in the experiment design process that feeders should be avoided for this reason. However, it was determined that without feeding the solidification shrinkage, the casting cope surface would form a sump, and suck into the casting. This made the measurements difficult. To avoid this, chill plates, shown in blue in Figure 1, were used at the cope surfaces to create a uniformly flat surface through rapid directional solidification. This resulted in the surface being in excellent condition for inclusion measurements.

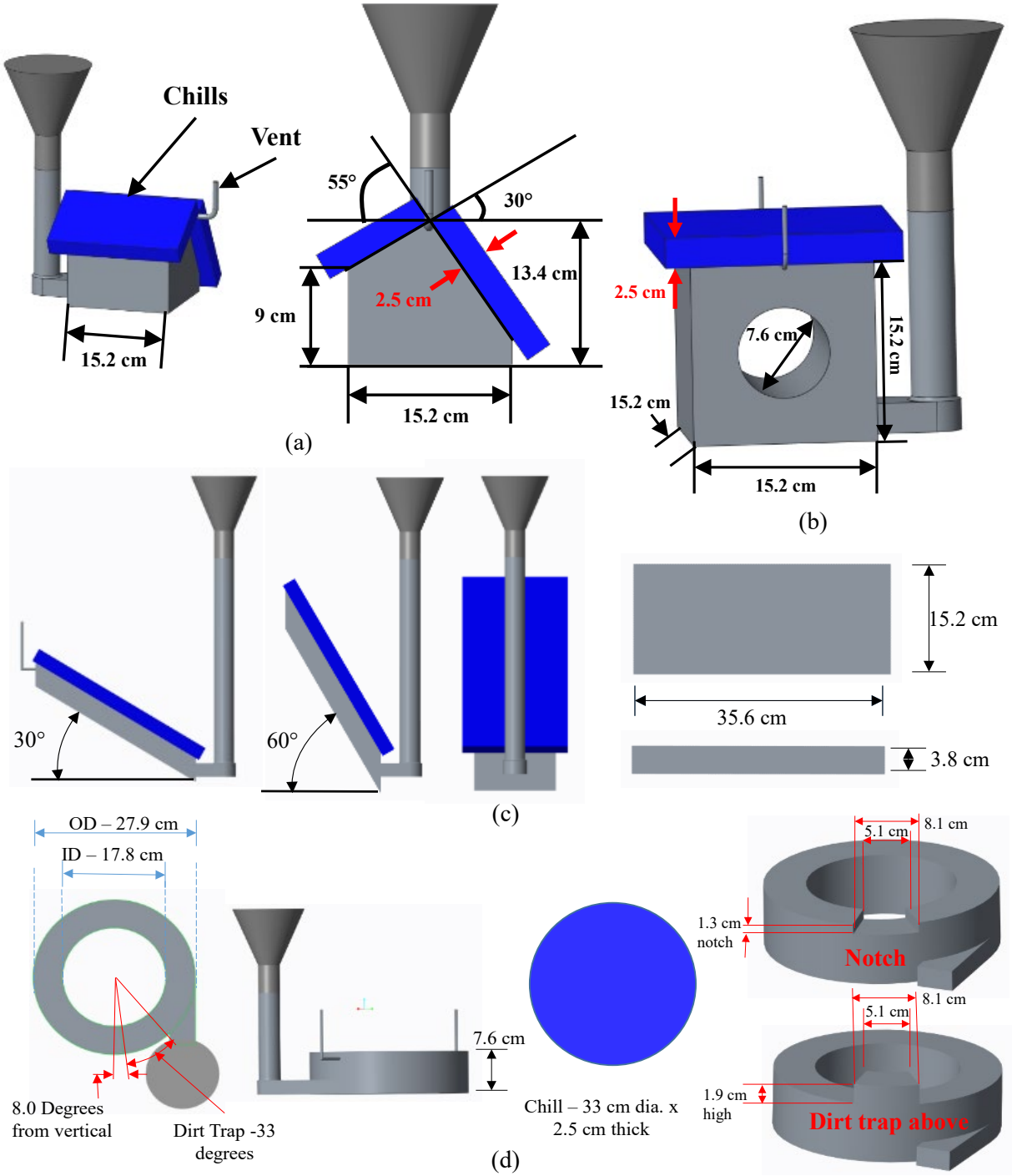

Figure 1. The six experiment cases simulated showing dimensions and other geometric features. Case A(a) has two inclined surfaces, case B (b) is an experiment with flow around a circular core, cases C1 and C2 (c) are plates inclined by 30° and 60°, and cases D1 and D2 have a ring flow pattern with a notch and dirt trap, respectively.

4. Comparison Between Simulations and Experiments

The images of, and data from, the inclusion analysis on the surfaces of the experimental and simulated castings are given in Figures 2 to 5. In these figures, the binary/black and white images of the inclusion sizes and locations on the chilled cope surfaces, and core surfaces for case B, are shown. Inclusion

locations are black. The red rectangles in the images indicate the ingate locations. The results of the image analyses of the inclusion distributions are given below the images. These results are inclusion area percentage (inclusion area/surface area), and inclusion count (number of individual/discrete inclusions) and the average equivalent diameter of the individual inclusions. For the simulation results, three of the four model parameters are constant; the mean inclusion diameter d_{inc} is 0.912 mm, the inclusion density ρ_{inc} is 3,230 kg/m^3 and the wall slip coefficient λ_{inc} is 0.025 cm. The total number of inclusions N_{inc} entering via the inlet was varied. The rational for varying N_{inc} was an observed effect of pouring order on the cleanliness of the melt for the lip pour ladle used. The pouring temperature and time simulated for each case are taken from thermocouple measurements and videos of the experiments, respectively. Model results for case A are shown in Figure 2(b) where the N_{inc} is 2000. For both measured and simulated results in Figure 2, case A has inclusions located at the upper ends of the surfaces at the "peak of the casting." The lower part of the casting was much cleaner by comparison for both results. The inclusion area percentages agree well for both cope surfaces. Inclusion counts are higher and sizes lower for the measurements compared to simulations. For the cored casting in case B, N_{inc} is again 2000. For case B in Figures 3(a) and 3(b), both measurements and simulations have a large amount of inclusions on the cope surface of the block with the inclusion locations biased on the ingate side of the casting. In Figures 3(b) and 3(d) the drag side at the core (top surface of the core) was almost entirely clean for both results. For the cope surface of the core (bottom side of core) in Figures 3(e) and 3(f), both results have numerous inclusions and the locations are biased at the mid-length of the core. For the two inclined plates (case C1 and C2) in Figure 4, both results have inclusion locations towards the bottom/ingate end of the plates. For case C1 N_{inc} is 4000, and N_{inc} is 2000 for C2. For the steeper inclined plate C2, both results have observably more inclusions distributed at the upper end of the plate in Figures 4(c) and 4(d). For both inclined plates the melt appears to be "cleaned" progressively as inclusions stick to the cope surface during filling. The ring flow cases D1 and D2 are shown in Figure 5. For case D1 N_{inc} is 4000, and N_{inc} is 500 for D2. The measurements showed that the dirt trap case D2 in Figure 5(c) had much fewer inclusions than the notch case D1 shown in Figure 5(a). Both the

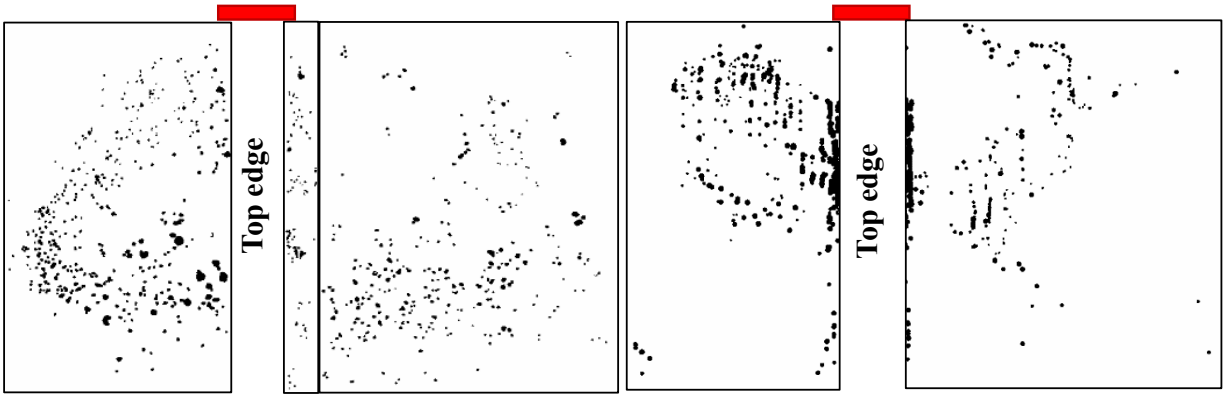

Measured Cope 1
Inclusion area 4.0%
Inclusion count 345
Average diam. 1.27 mm

Measured Cope 2
Inclusion area 2.0%
Inclusion count 280
Average diam. 1.13 mm

(a)

Simulated Cope 1
Inclusion area 4.39%
Inclusion count 156
Average diam. 1.97 mm

Simulated Cope 2
Inclusion area 2.17%
Inclusion count 129
Average diam. 1.75 mm

(b)

Figure 2. Comparison between measured inclusion data in case A (a) and simulation results (b).

measured dirt trap and the notch cases were cleaner upstream of the notch and trap features compared to downstream of them. The simulations in Figures 5(b) and 5(d) had the opposite distribution with more inclusions upstream than downstream.

A summary of the comparisons between measured and simulated inclusion data is given for the inclusion area percentage in Figure 6(a) and also for the inclusion count in Figure 6(b). The nine points in each plot correspond to the surfaces plotted in Figures 2 to 5. In Figure 6(a) the inclusion area

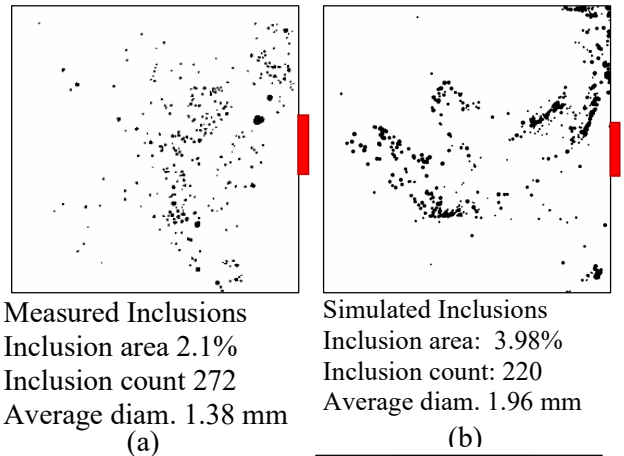

Measured Inclusions
Inclusion area 2.1%
Inclusion count 272
Average diam. 1.38 mm
(a)

Simulated Inclusions
Inclusion area: 3.98%
Inclusion count: 220
Average diam. 1.96 mm
(b)

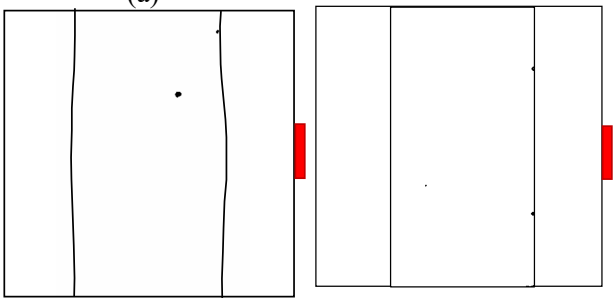

Measured Core Top
Inclusion area 0.05%
Inclusion count 2
Average diam. 2.36 mm
(c)

Simulated Core Top
Inclusion area 0.05%
Inclusion count 5
Average diam. 1.44 mm
(d)

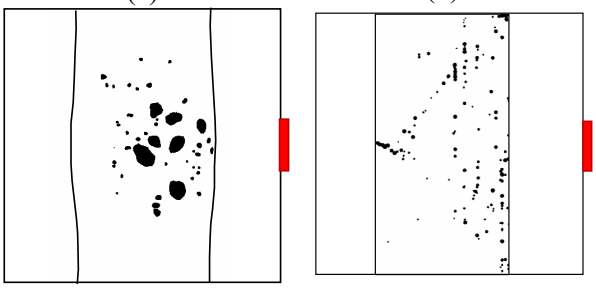

Measured Core Bottom
Inclusion area 3.2%
Inclusion count 45
Average diam. 3.19 mm
(e)

Simulated Core Bottom
Inclusion area 1.72%
Inclusion count 105
Average diam. 1.77 mm
(f)

Figure 3. Comparison between measured and simulated inclusion data for case B. Measured cope surface (a) and simulation results (b). Measured core top surface (c) and simulation (d). Measured core bottom surface (e) and simulation (f).

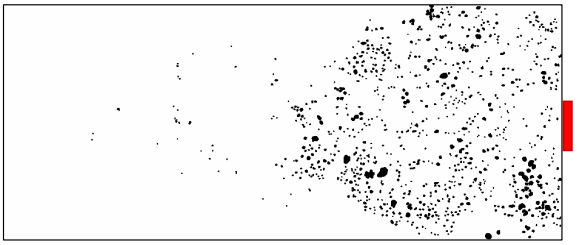

Measured Inclusions
Inclusion area 3.6%
Inclusion count 837
Average diam. 1.55 mm
(a)

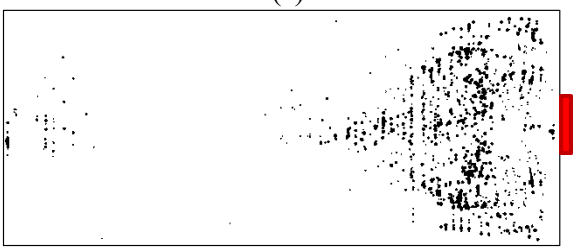

Simulated Inclusions
Inclusion area 3.86%
Inclusion count 483
Average diam. 1.99 mm
(b)

Measured Inclusions
Inclusion area 1.9%
Inclusion count 496
Average diam. 1.54 mm
(c)

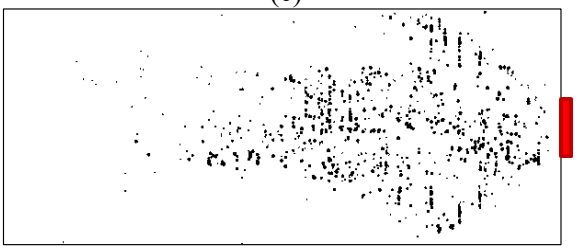

Simulated Inclusions
Inclusion area 3.4%
Inclusion count 506
Average diam. 2.0 mm
(d)

Figure 4. Comparison between measured and simulated inclusion data for cases C1 and C2. Measured case C1 cope surface (a) and simulation results (b). Measured case C2 cope surface (c) and simulation (d) results.

percentage shows an excellent trend over the range of values and remarkable agreement between measurement and simulation. The inclusion count in Figure 6(b) shows a good trend between the experiment and model, but the simulations appear to consistently under predict the inclusion count. The

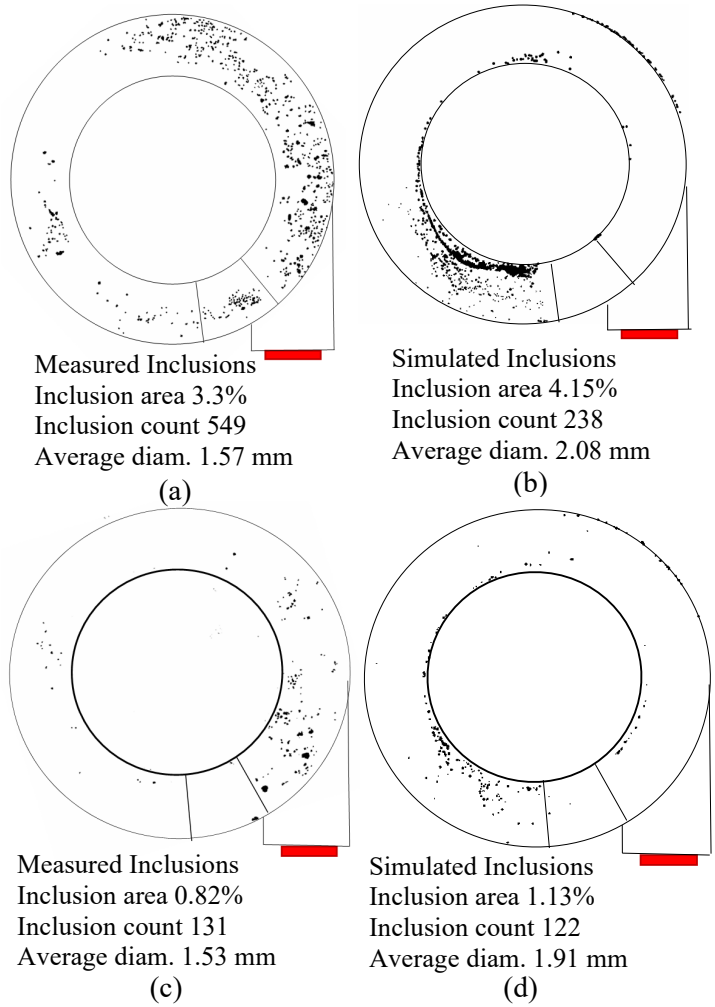

Figure 5. Comparison between measured and simulated inclusion data for cases D1 and D2. Measured case D1 cope surface (a) and simulation results (b). Measured case D2 cope surface (c) and simulation (d) results.

mean inclusion diameter did not predict a trend with the simulation diameter range being from 1.4 to 2.1 mm and the measured range from 1.1 to 3.2 mm.

5. Conclusions

Results from a model are presented that predicts the motion and final locations of oxide inclusions in steel castings. The simulations use a distribution of inclusions entering the casting system via the inlet stream, ranging in size from 50% to 150% of a prescribed mean diameter. Upon entering the casting system with the filling flow, the inclusions are transported with the flow under the effects of buoyancy and drag to their final locations in the solidifying casting. Model results are compared to experimental measurements results on nine surfaces of five casting experiments. A mean inclusion diameter of 0.91 mm is used in the simulation results given here. The inclusion density used is 3,230 kg/m^3 and the wall slip coefficient is 0.025 cm. The total number of inclusions entering via the inlet was varied from 500 to 4000 inclusions entering the casting during the filling process. Comparisons are made between the measured and simulated inclusion area coverage, inclusion count/number and the average diameter on the casting surfaces, and the standard errors in the model results are 1.0%, 179,

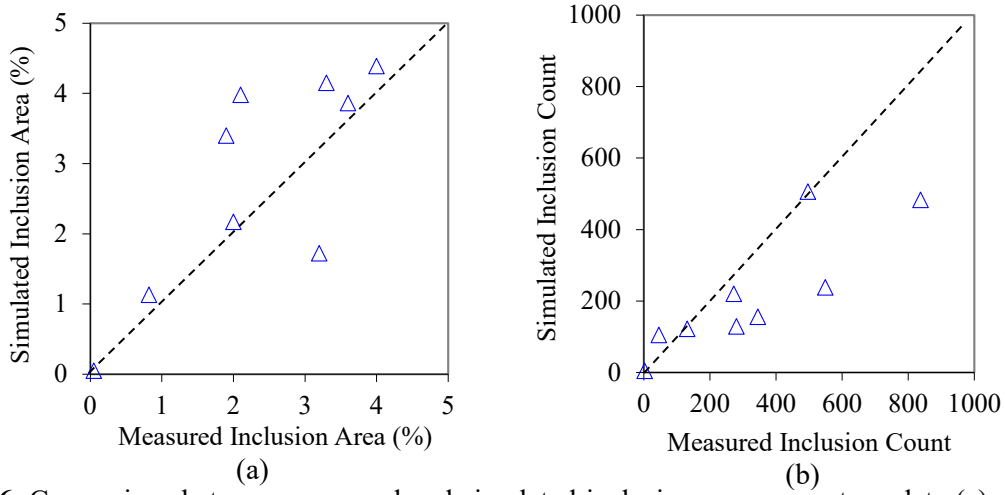

Figure 6. Comparison between measured and simulated inclusion area percentage data (a) and count (b) for all cases.

and 0.67 mm, respectively, compared to the measurements. For the 30 and 60 degree inclined plate cases, the measurements and simulations showed more inclusions near the lower end of the plates. The inclusions entering the casting system were cleaned from the melt as these cases filled. For the cored casting, both measured and simulation results had clean core top surfaces and dirty core bottom surfaces. In order to verify the modeling capability of predicting final inclusion locations, many repeated experiments of the cases presented here would be needed. However, the model results presented compare well with the experiments overall in predicting the area coverage on the casting surfaces. This demonstrates the model's usefulness in designing filling systems that provide cleaner melt flow by transporting inclusions to less harmful locations in the casting system.

Acknowledgements
This research is sponsored by the DLA-Troop Support, Philadelphia, PA and the Defense Logistics Agency Information Operations, J68, Research & Development, Ft. Belvoir, VA.

References
[1] Svoboda J, Monroe R, Bates C and Griffin J 1987 *AFS Trans.* **95** 187-202
[2] Griffin J and Bates C 1991 *Ladle Treating Pouring and Gating for the Production of Clean Steel Castings* (Steel Founders' Society of America Research Report No. 104)
[3] Melendez A, Carlson K, and Beckermann C 2010 *Int. J. Cast Metals Res.* **23** 278-88
[4] Donahue R, Hardin R and Beckermann C 2021 *Proc. of the 75th SFSA Technical and Operating Conf.* (Chicago IL: Steel Founders' Society of America) Paper No. 4.11
[5] Majidi S, Beckermann C, Fainberg, J, Schaefer W, and Bodenburg M 2018 *Mat. Sci. Forum* **925** 419-26
[6] Schindelin J, Arganda-Carreras I and Frise E 2012 *Nature Methods* **9** 676-82